Cukurova Medical Journal
ÇUKUROVA ÜNİVERSİTESİ TIP FAKÜLTESİ

Cukurova Med J 2026;51(2):486-496
DOI: 10.17826/cumj.1901420

RESEARCH

Imaging features of metastases to the breast from extramammary non-hematological malignancies: a BI-RADS v2025 descriptive study

Meme dışı hematolojik olmayan malignitelerden memeye yayılan metastazların görüntüleme özellikleri: BI-RADS v2025 uyarınca yapılmış bir tanımlayıcı çalışma

Umur Anıl Pehlivan[1], Hülya Özdemir[1]

[1] Başkent University, Adana, Türkiye

Abstract

Purpose: The aim of this study was to evaluate the imaging features of metastases to the breast from extramammary non-hematological malignancies, by applying the updated descriptors and assessment categories of the ACR BI-RADS v2025 Manual.
Materials and Methods: In this single-center descriptive study, 22 patients with histopathologically confirmed metastases to the breast from solid tumors were evaluated. Mammography (MG) was performed in 10 cases, ultrasound (US) in all cases, and magnetic resonance imaging (MRI) in one. Subsequently, all modalities were reviewed by two radiologists in consensus. Lesion morphology and BI-RADS category were reassessed according to the BI-RADS v2025.
Results: The most common primary tumors were lung (n=7, 31.8%) and ovarian (n=5, 22.7%) carcinomas. Clinical presentation was predominantly unilateral (81.8%) and solitary (54.5%). Regarding MG findings, mass lesions (80%) and non-mass focal asymmetries (20%) were identified; furthermore, the most frequent mass morphology was a lobulated shape (n=4) with obscured margin (n=4). Notably, internal calcifications were absent in 100% of the cases. US evaluation revealed 21 masses and one non-mass lesion. Among mass lesions, the most common features were a lobulated shape (n=9), hypoechogenicity (n=15), and indistinct margin (n=10). Notably, an echogenic rind was identified in 63.6% of lesions, and posterior acoustic enhancement was present in 54.5%. Internal and/or peripheral vascularity was detected in 83.3% of lesions evaluated with Doppler US. Elastography showed hard (47.6%) and intermediate (52.4%) stiffness. The patient who underwent MRI had a circumscribed T2-hyperintense mass with thick rim-enhancement and diffusion restriction.

Öz

Amaç: Bu çalışmanın amacı meme dışı hematolojik olmayan malignitelerin memeye metastazlarının görüntüleme özelliklerini, ACR BI-RADS v2025 Kılavuzu'nun güncellenmiş tanımlayıcılarını ve değerlendirme kategorilerini uygulayarak değerlendirmektir.
Gereç ve Yöntem: Bu tek merkezli tanımlayıcı çalışmada, solid tümörlerden kaynaklanan ve histopatolojik olarak doğrulanmış memeye metastazı olan 22 hasta değerlendirildi. 10 vakada mamografi (MG), tüm vakalarda ultrasonografi (US) ve bir vakada manyetik rezonans görüntüleme (MRG) yapıldı. Takiben, tüm modaliteler iki radyolog tarafından beraber incelendi. Lezyon morfolojisi ve BI-RADS kategorisi, BI-RADS v2025'e göre yeniden değerlendirildi.
Bulgular: En sık izlenen primer tümörler akciğer (n=7, %31,8) ve over (n=5, %22,7) karsinomlarıydı. Klinik prezentasyon ağırlıklı olarak tek taraflı (%81,8) ve soliter (%54,5) idi. MG bulguları açısından; kitle lezyonları (%80) ve kitle dışı fokal asimetriler (%20) tanımlandı; ayrıca, en sık kitle morfolojisi lobüle şekil (n=4) ve örtülü marjin (n=4) olarak saptandı. Dikkat çekici şekilde, vakaların %100'ünde iç kalsifikasyon izlenmedi. US değerlendirmesinde 21 kitle ve bir kitle dışı lezyon saptandı. Kitle lezyonları arasında en yaygın özellikler lobüle şekil (n=9), hipoekojenite (n=15) ve belirsiz marjin (n=10) idi. Özellikle, lezyonların %63,6'sında ekojenik kabuk tanımlandı ve %54,5'inde posterior akustik güçlenme mevcuttu. Doppler US ile değerlendirilen lezyonların %83,3'ünde internal ve/veya periferik vaskülarite saptandı. Elastografi, sert (%47,6) ve orta (%52,4) düzeyde sertlik gösterdi. MRG yapılan hastada, kalın rim tarzında kontrastlanan ve difüzyon kısıtlaması gösteren, T2-hiperintens, düzgün sınırlı kitle mevcuttu.

Address for Correspondence: Umur Anıl Pehlivan, Department of Radiology, Başkent University Faculty of Medicine, Adana Dr. Turgut Noyan Application and Research Center, Adana, Türkiye
Received: 02.03.2026 Accepted: 26.04.2026

Conclusion: According to the updated BI-RADS v2025 Manual, metastases to the breast from solid tumors frequently present as lobulated masses with indistinct or obscured margin. The absence of microcalcifications is a key feature favoring metastasis over primary breast carcinoma, except in rare psammomatous ovarian carcinoma. The high prevalence of an echogenic rind and the presence of non-mass focal asymmetries are critical diagnostic clues that should not be overlooked, particularly in dense breast parenchyma.
Keywords: Breast neoplasm, differential diagnosis, metastasis, ultrasonography, mammography.

Sonuç: Güncellenmiş BI-RADS v2025 Kılavuzu'na göre, solid tümörlerden memeye yayılan metastazlar sıklıkla sınırları belirsiz veya örtülü marjinli, lobüle kitleler şeklinde görülür. Mikrokalsifikasyonların bulunmaması, nadiren görülen psammomatöz over karsinomu hariç olmak üzere, primer meme karsinomuna kıyasla metastazı düşündüren temel bir bulgudur. Ekogenik kabuğun yüksek prevalansı ve kitle dışı fokal asimetrilerin varlığı, özellikle yoğun meme parankiminde göz ardı edilmemesi gereken kritik tanısal ipuçlarıdır.
Anahtar kelimeler: Ayırıcı tanı, mamografi, meme neoplazmı, metastaz, ultrasonografi.

INTRODUCTION

Breast cancer is the most common primary malignancy in women and the leading cause of cancer-related death among the female population worldwide[1]. While the vast majority of malignant breast neoplasms consist of primary epithelial carcinomas, metastasis to the breast is an infrequent clinical occurrence. Among these, the most common source is a contralateral primary breast carcinoma, followed by hematological malignancies and various systemic carcinomatous metastases such as melanoma, lung cancer, ovarian cancer, and others[2-4]. In general, extramammary metastases to the breast signify disseminated systemic disease and are consequently associated with a poor prognosis[3,5].

The reported incidence of metastases to the breast in the literature remains inconsistent, primarily due to discrepancies between clinical and autopsy-based data, as well as the variable inclusion of hematological malignancies across studies. As a result, secondary breast lesions are estimated to account for 0.1% to 6.6% of all malignant mammary tumors[3,6-9]. Current epidemiological data suggest that hematological involvement is now encountered more frequently than systemic solid tumor metastases. This shift may be attributed to the rising global incidence of hematological disorders and the improved efficacy of early detection protocols for solid tumors, which facilitates intervention before distant dissemination to the breast occurs[2]. Specifically, the incidence of metastases to the breast originating from extramammary non-hematological malignancies is remarkably low, estimated at less than 1% of all breast malignancies[4,10].

The clinical and radiological presentations of metastases to the breast are highly heterogeneous and can mimic primary breast carcinomas or benign entities[5,10]. This variability hinders the ability to generalize specific imaging characteristics of the disease. Such diagnostic overlap necessitates meticulous clinical assessment, particularly in patients with a documented oncological history. Precise differentiation is vital because management protocols diverge significantly; whereas the standard of care for primary breast cancer typically involves surgical resection with or without adjuvant therapies, metastatic lesions are generally managed through systemic treatment protocols[5]. Consequently, a high index of suspicion and familiarity with common imaging manifestations are crucial to prevent unnecessary surgical procedures and ensure timely initiation of appropriate therapy.

Although the imaging features of metastatic breast involvement have been documented in the literature both prior to and following the formalization of the Breast Imaging Reporting and Data System (BI-RADS), there is a notable absence of studies evaluated using the recently released American College of Radiology (ACR) BI-RADS v2025 Manual[5,11-14]. This latest guideline introduces minor yet significant updates[15]. The unique contribution of this study to the literature lies in its being the first to re-evaluate extramammary non-hematological breast metastases through the lens of the most current ACR BI-RADS v2025 descriptors. Our central hypothesis is that despite the heterogeneous presentation of metastatic lesions, the new BI-RADS v2025 Manual will provide a more precise framework for identifying specific imaging patterns, thereby aiding in the critical differentiation between primary and secondary breast malignancies. The aim of the present descriptive study is to evaluate the radiological findings of metastases to the breast from extramammary non-hematological malignancies according to the updated BI-RADS v2025 descriptors and classification standards.

MATERIALS AND METHODS

Study design

This descriptive, single-center study was conducted at the Department of Radiology, Division of Breast Imaging, Baskent University Faculty of Medicine Adana Dr. Turgut Noyan Application and Research Center, a tertiary-level academic hospital specialized in oncological imaging.

The study protocol was approved by the Baskent University Institutional Review Board (Project No: KA26/74; approval date: 18 February 2026). Data integrity and patient confidentiality were ensured through the hospital's secure Electronic Medical Record (EMR) system and a dedicated, high-resolution Picture Archiving and Communication System (PACS) specifically optimized for diagnostic imaging. All procedures were performed in accordance with the Declaration of Helsinki.

Sample

Between January 2010 and February 2026, patients who underwent ultrasound (US) guided core needle breast biopsy procedures at our institution were identified (n=4,875). The inclusion criteria were clinical and radiological suspicion of breast involvement and histopathological confirmation of metastasis from an extramammary malignancy (n=50). Exclusion criteria were: (1) hematological malignancies (n=25) and (2) insufficient retrospective PACS images for reliable evaluation (n=3). Consequently, the final study cohort consisted of 22 patients with confirmed diagnoses (Figure 1).

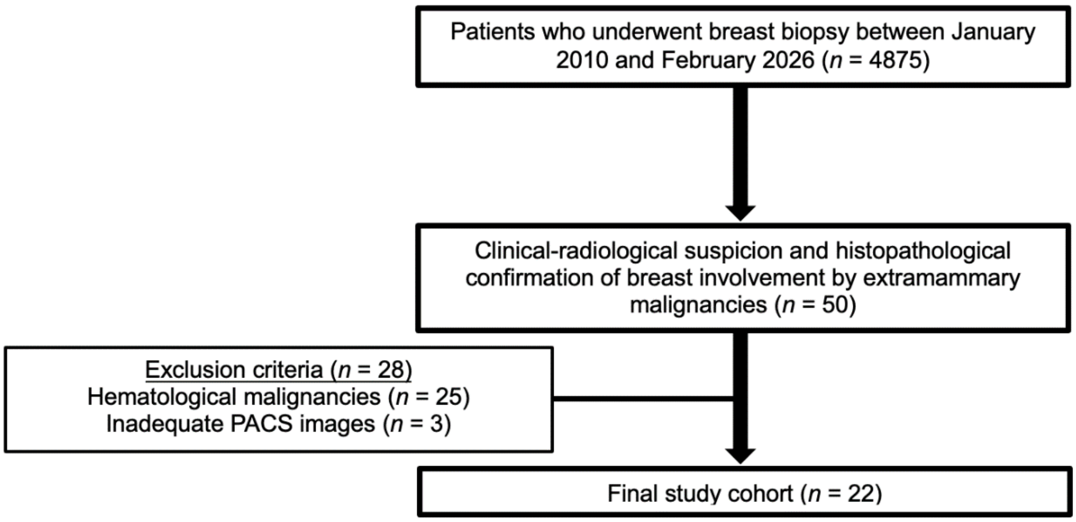

Figure 1. Study flowchart of patient selection.
PACS, Picture Archiving and Communication System.

Procedure

Demographic variables, including age and gender, as well as histopathological subtypes of the primary tumor origin, were obtained from the hospital's EMR system.

Imaging protocols and technical equipment

All imaging data were retrospectively retrieved and analyzed via PACS. Mammography (MG) evaluations in craniocaudal and mediolateral oblique projections were available for 10 patients; these were performed using a Mammomat Inspiration system (Siemens Healthineers, Erlangen, Germany). US was performed on all patients using two identical Acuson S2000 devices (Siemens Healthineers, Erlangen, Germany). Color and/or power Doppler US was available for 12 patients, whereas shear-wave and/or strain elastography was performed in 21 patients. Magnetic resonance imaging (MRI), including dynamic contrast-enhanced and diffusion-weighted sequences, was conducted in one patient using a 1.5-Tesla MAGNETOM Avanto system (Siemens Healthineers, Erlangen, Germany). Institutional standardized scanning protocols were strictly followed for each modality to ensure technical consistency across the study period.

Image analysis

All imaging studies were reviewed in consensus by two radiologists certified with the European Diploma in Radiology (EDiR), possessing three and 15 years of specialized experience in breast imaging, respectively. To ensure reliability and minimize diagnostic bias, both reviewers were blinded to the initial radiological reports, although they were provided with the patients' primary oncological history as per clinical routine. Final assessments were performed in accordance with the ACR BI-RADS v2025 Manual. Evaluated parameters included lesion lateralization, number of lesions, axillary lymph node status (absent or present), and evidence of cutaneous involvement. The biopsied lesion was designated as the target (dominant) lesion, and its maximum diameter was recorded. The ACR BI-RADS v2025 Manual represents a comprehensive update to the fifth edition (2013), introducing several revisions that are directly relevant to the present study's image analysis. The most impactful change for this investigation is the reinstatement of the lobulated shape descriptor across all three modalities (MG, US, and MRI), which had been eliminated in the fifth edition to prevent confusion with the margin term microlobulated. In v2025, the term lobulated (replacing the fourth edition's lobular) is formally defined as a distinct shape category, allowing more precise morphological characterization of masses with undulating contours. Additionally, v2025 introduces the non-mass lesion as a formal US finding — defined as a discrete finding seen in three dimensions without the discrete margination of a mass. ACR BI-RADS v2025 also formalizes the echogenic rind as a named sub-finding under associated features, representing the echogenic tissue directly surrounding a lesion. Terminology revisions relevant to our assessment also include: non-circumscribed (replacing not circumscribed) and non-parallel (replacing not parallel) for margin and orientation descriptors, respectively; mixed solid and cystic replacing complex cystic and solid for echo pattern; and the renaming of absent vascularity to avascular. In MRI, T2 signal intensity is introduced as a new mass sub-finding with dedicated descriptors (hyperintense and not hyperintense), and thick rim enhancement replaces the previously used rim enhancement descriptor. Final lesion characterization and BI-RADS assignment were performed according to the ACR BI-RADS v2025 Manual[15].

Statistical analysis

Due to the retrospective and descriptive nature of this study and the rarity of the clinical entity, with extramammary non-hematological metastases accounting for less than 1% of all breast malignancies, a formal power analysis was not performed. Instead, a total population sampling (complete enumeration) approach was adopted, identifying all consecutive patients meeting the inclusion criteria over a 16-year period (2010–2026). This approach was chosen to maximize the descriptive power and reflect the full radiological spectrum of this rare condition at a tertiary referral center. The distribution of continuous variables, such as age and lesion size, was evaluated for normality using the Shapiro-Wilk test. Since these variables followed a non-normal distribution, continuous data were expressed as medians with ranges (minimum–maximum). Categorical variables, including all ACR BI-RADS v2025 descriptors, were summarized as absolute frequencies and percentages. As this was a single-arm descriptive study without a control group, comparative inferential statistics (e.g., p-value calculations) were not applicable; instead, frequency distribution analysis was utilized to characterize the most prevalent imaging patterns of the metastatic lesions.

RESULTS

The study cohort comprised 22 patients, including 19 females (86.4%) and three males (13.6%), with a median age of 53 years (range: 17–83 years). The primary sources of extramammary non-hematological malignancies were diverse; notably, lung carcinoma was the most prevalent (n=7), followed by ovarian carcinoma (n=5), pancreatic neuroendocrine tumor (n=2), and renal cell (n=2) carcinomas. Additionally, single instances (n=1 each) of malignant melanoma, rhabdomyosarcoma, malignant mesenchymal tumor, Ewing's sarcoma, adrenocortical carcinoma (ACC), and cholangiocellular carcinoma (CCC) were identified. The distribution of the originating tumors of the metastasis to the breast is presented in Table 1.

Table 1. The distribution of the primary tumor sites

Primary tumor site	n
Lung carcinoma	7
Ovarian carcinoma	5
Pancreatic neuroendocrine tumor	2
Renal cell carcinoma	2
Malignant melanoma	1
Rhabdomyosarcoma	1
Malignant mesenchymal tumor	1
Ewing's sarcoma	1
Adrenocortical carcinoma	1
Cholangiocellular carcinoma	1

Table 2. Mammography findings of metastatic lesions to the breast.

Parameter	Finding	n (%)
Lesion type	Mass	8 (80%)
	Non-mass (focal asymmetry)	2 (20%)
	with architectural distortion	1
	with skin thickening	1
Mass shape (n = 8)	Lobulated	4 (50%)
	Round	2 (25%)
	Oval	1 (12.5%)
	Irregular	1 (12.5%)
Mass margin (n = 8)	Obscured	4 (50%)
	Indistinct	2 (25%)
	Circumscribed	2 (25%)
Mass density (n = 8)	Equal density	4 (50%)
	High density	4 (50%)
Calcifications	Absent	10 (100%)

n: number of dominant lesions.

Three patients had no known malignancy at the time metastasis to the breast was diagnosed, whereas the remaining patients had previously been diagnosed with a primary cancer. In 10 patients, breast imaging was performed because of clinical symptoms such as a palpable breast mass, pain, edema, or axillary lymphadenopathy, and the diagnosis of metastasis to the breast was established following imaging examinations and biopsy. In the other 12 patients, the lesions were detected incidentally, most commonly during routine follow-up with positron emission tomography/computed tomography or during staging imaging for the primary malignancy; subsequently, breast imaging modalities and biopsies were performed.

Metastatic involvement was predominantly unilateral (81.8%), while four patients exhibited bilateral disease (18.2%). Regarding lesion multiplicity, a solitary mass was the most frequent finding (54.5%, n=12). Multifocality or multicentricity was noted in the remaining cases: five patients presented with two lesions, three with three lesions, and two with more than three lesions.

The majority of the cohort (n=15; 68.2%) showed no evidence of axillary lymphadenopathy on imaging, whereas seven patients (31.8%) presented with ipsilateral or bilateral axillary nodal involvement. Cutaneous manifestations, such as skin thickening or direct invasion, were exceptionally rare, occurring in only a single patient (4.5%) who presented with diffuse involvement and bilateral skin thickening.

The median diameter of the dominant lesions was 18 mm (range: 7–49 mm). According to the BI-RADS density classification, the most prevalent parenchymal pattern was Category C (n=4), followed by Category A (n=3) and Category B (n=3) on MG. The target lesions presented as masses in eight patients (80%) (Figure 2, Figure 3), while the remaining two patients (20%) exhibited non-mass findings characterized by focal asymmetry (Figure 4). Among the non-mass lesions, associated findings included focal architectural distortion in one patient and skin thickening in the other. Of the lesions demonstrating non-mass characteristics, one was classified as BI-RADS category C, while the other was categorized as BI-RADS category B. Regarding the eight mass lesions, the most frequent morphology was a lobulated shape (n=4), followed by round (n=2), oval (n=1), and irregular (n=1) shapes. Margin characteristics were classified as obscured (n=4), indistinct (n=2), and circumscribed (n=2). The mass lesions demonstrated equal density (n=4) or high density (n=4) relative to the surrounding parenchyma. Notably, internal calcifications were absent in all 10 cases evaluated by MG. All mammographic findings are summarized in Table 2.

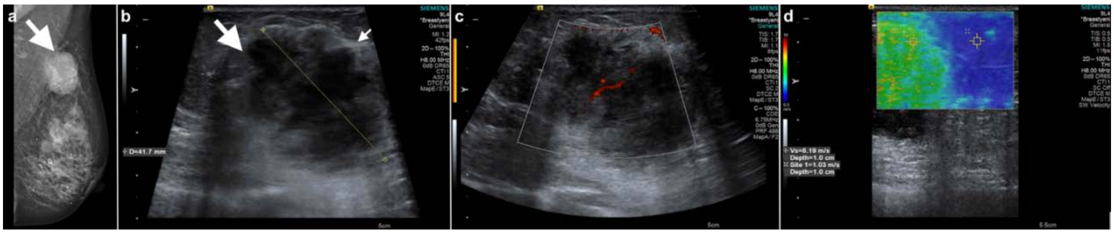

Figure 2. A 66-year-old female with metastasis from lung cancer. On the left mediolateral oblique mammogram (a), a mass lesion (arrow) with a lobulated shape, obscured margin, and equal density is observed. On breast ultrasound (b), a hypoechoic mass (arrow) with a lobulated shape, indistinct margin, and parallel orientation is seen, demonstrating posterior acoustic enhancement and echogenic rind (short arrow). On Power Doppler ultrasound (c), the lesion shows internal vascularity. Shear-wave elastography (d) demonstrates that the lesion has intermediate stiffness.

Figure 3. An 83-year-old female with breast metastasis from adrenocortical carcinoma. Right craniocaudal (a) and mediolateral oblique (b) mammograms demonstrate a round-shape mass with an obscured margin and high density. B-mode and Virtual Touch Tissue Image (c), shear-wave elastography (d) demonstrate hypoechoic lobulated-mass with an angular margin, parallel orientation, and hard stiffness.

Figure 4. A 46-year-old woman with breast metastasis from ovarian cancer. Right craniocaudal (a) and mediolateral oblique (b) mammograms demonstrate focal asymmetry (arrow) associated with skin thickening (curved arrow). On B-mode ultrasound (c), a non-mass lesion (arrowhead) with a heterogeneous echotexture and segmental distribution is observed, showing an echogenic rind (short arrows) and skin thickening (curved arrow). Elastography (d) demonstrates intermediate stiffness of the lesion.

Figure 5. A 40-year-old female patient with breast metastasis from cholangiocellular carcinoma. B-mode ultrasound (a) reveals a lobulated-shape mass with indistinct margin and echogenic rind (curved arrows). Shear-wave elastography (b) shows that the mass has high stiffness.

Table 3. Ultrasound findings of metastatic lesions to the breast.

Parameter	Finding	n (%)
Lesion type	Mass	21 (95.5%)
	Non-mass	1 (4.5%)
Mass characteristics		
Shape (n = 21)	Lobulated	9 (42.9%)
	Oval	6 (28.6%)
	Round	3 (14.3%)
	Irregular	3 (14.3%)
Margin (n = 21)	Indistinct	10 (47.6%)
	Circumscribed	4 (19.0%)
	Angular	4 (19.0%)
	Microlobulated	2 (9.5%)
	Spiculated	1 (4.8%)
Orientation (n = 21)	Parallel	17 (80.9%)
	Non-parallel	4 (19.1%)
Internal echogenicity (n = 21)	Hypoechoic	15 (71.4%)
	Hyperechoic	3 (14.3%)
	Heterogeneous	3 (14.3%)
Associated features		
Posterior acoustic features (n = 22)	Enhancement	12 (54.5%)
	No posterior features	10 (45.5%)
Echogenic rind / pseudocapsule (n = 22)	Echogenic rind	14 (63.6%)
	Pseudocapsule	0 (0%)
Vascularity — Color/Power Doppler (n = 12)*	Internal and/or peripheral vascularity	10 (83.3%)
	Avascular	2 (16.7%)
Elastography — strain/shear wave elastography (n = 21)*	Hard stiffness	10 (47.6%)
	Intermediate stiffness	11 (52.4%)

n: number of dominant lesions; * Available for a subset of lesions only.

US evaluation of the 22 dominant lesions revealed 21 masses (Figure 2, Figure 3, Figure 5). The remaining one presented as a non-mass lesion (Figure 4). The most prevalent shape among the mass lesions was lobulated (n=9), followed by oval (n=6), round (n=3), and irregular (n=3). Margin analysis showed that an indistinct margin was the most frequent finding (n=10), followed by circumscribed (n=4), angular (n=4), microlobulated (n=2), and spiculated (n=1) margins. Regarding orientation, 17 mass lesions (80.9%) exhibited a parallel orientation, while four (19.1%) were non-parallel. The internal echo pattern was predominantly hypoechoic (n=15), whereas hyperechoic (n=3) and heterogeneous (n=3) patterns were less common.

The single non-mass lesion was characterized by a heterogeneous echo pattern with a segmental distribution. Evaluation of posterior acoustic features showed posterior enhancement in 12 dominant lesions (54.5%), while the remaining 10 lesions (45.5%) exhibited no posterior features. Notably, an echogenic rind was identified in 14 of the 22 metastatic lesions (63.6%), whereas no pseudocapsule was detected. Color or power Doppler US was available for 12 dominant lesions, of which 10 (83.3%) demonstrated internal and/or peripheral vascularity. Strain and/or shear-wave elastography assessment (n=21) showed hard stiffness in 10 dominant lesions and intermediate stiffness in 11 dominant lesions. All sonographic findings are summarized in Table 3.

MRI was performed in a single case involving a patient with primary ovarian carcinoma. The target lesion was characterized as an oval, circumscribed mass exhibiting T2-hyperintensity and a thick rim-enhancement pattern. Furthermore, the lesion demonstrated marked diffusion restriction, with an apparent diffusion coefficient (ADC) value of 0.700×10^{-3} mm²/s.

The most common BI-RADS assignment was 4B (n=13), followed by 4C (n=3), 4A (n=3), 5 (n=2), and 3 (n=1), respectively.

DISCUSSION

Metastasis to the breast is a clinical rarity that poses a significant diagnostic challenge. The present study represents the first descriptive analysis of this rare entity evaluated within the ACR BI-RADS v2025 framework. Our findings reinforce several classical imaging paradigms while identifying critical terminological shifts that may influence future diagnostic accuracy.

The distribution of primary malignancies metastasizing to the breast in the present study reflects the specific oncologic referral patterns; notably, lung and ovarian carcinomas were the most frequent sources, which is consistent with the study by Wan et al.[16]. In contrast, while some studies describe malignant melanoma as the most common source, it was identified in only a single patient in our series[3,13,17]. Interestingly, our cohort also included cases of Ewing's sarcoma and CCC, both of which have only been documented in sporadic case series and pictorial reviews[5,6,8,14,18,19]. In addition, one exceptionally rare case of ACC metastasis to the breast was documented in the current cohort.

A predominance of unilateral involvement has been consistently reported in the literature[3,14,16], which aligns with the similarly high rate of unilaterality observed in the present study. With regard to lesion multiplicity, our findings are concordant with prior reports[16,17], in which solitary metastases constituted the most common presentation. An exception is the study by Surov et al.[3], which documented a notably higher frequency of multiple lesions. The rate of axillary lymphadenopathy in our cohort was compatible with the 35.7% prevalence reported by Wan et al.[16]. Furthermore, cutaneous involvement was rare (4.5%) in the present study, consistent with prior reports[3,11,13].

Classically metastases to the breast from solid extramammary malignancies have been described on MG as round or oval masses with circumscribed margin, lacking the spiculated configuration typically associated with primary breast cancer[12,14]. Conversely, our series demonstrated a predominance of lobulated to round shape with obscured or indistinct margin, reflecting a somewhat different morphologic spectrum than that emphasized in earlier reports. The relatively high prevalence of obscured and indistinct margin in our cohort frequently encountered in dense breast parenchyma (BI-RADS Category C; n=4) suggests that the well-circumscribed margin described in several reviews may be partially masked by adjacent fibroglandular tissue[6,14]. Moreover, the reinstatement of the lobulated shape descriptor in BI-RADS v2025 enhanced diagnostic precision, enabling accurate classification of lesions previously forced into oval or irregular categories[3,18,20].

Although the literature predominantly focuses on mass lesions, non-mass morphologies were also identified in a subset of MG examinations. The study by Noguera et al., after excluding patients diagnosed with hematologic malignancies, contralateral breast cancer metastases, and cases evaluated solely by computed tomography, 18 patients with MG available for evaluation of solid extramammary metastases remained[17]. Noguera et al. reported inflammatory changes in three cases and focal asymmetry in one case; when reclassified according to the BI-RADS v2025 Manual, these findings would appropriately fall under category of asymmetries[17]. In our study, non-mass findings accounted for 20% of MG presentations, underscoring the importance of recognizing these subtle abnormalities particularly in dense breasts, where a discrete mass may not yet be evident. Additionally, the absence of microcalcifications in all MG cases in our cohort represents a characteristic feature of metastatic disease and is in keeping with the existing literature, which indicates that calcifications are exceedingly rare unless the primary tumor is a psammomatous ovarian carcinoma[14].

This study demonstrated a predominance of hypoechoic mass lesions with indistinct margin and lobulated shapes on US. Notably, the 45.5% rate of ill-circumscribed margin reported in the extramammary solid tumor metastasis subgroup of Noguera et al.'s study (following reanalysis excluding patients diagnosed with hematologic malignancies and contralateral primary breast cancers) is compatible with our findings, whereas the 92.9% rate of indistinct margin reported by Wan et al. is substantially higher than that observed in our cohort[16,17]. Specifically, Noguera et al. and Wan et al. reported irregular shapes in 45.5% and 92.9% of their cases, respectively, proportions significantly higher than those in our analysis[16,17]. This discrepancy is likely attributable to the absence of the lobulated shape descriptor in the fifth edition of BI-RADS, which may have necessitated the categorization of lobulated metastases into less precise categories, such as irregular or oval[15]. According to the BI-RADS v2025, lesions previously categorized as irregular may either remain classified as irregular or be redefined as lobulated. This observation underscores how successive revisions of BI-RADS can influence the reported prevalence of specific morphologic features in retrospective comparative analyses. However, the increasing recognition in recent studies of lesions lacking benign imaging features reinforces the notion that secondary breast malignancies frequently deviate from the traditionally described well-circumscribed morphology historically attributed to them; future prospective investigations will further elucidate this issue. Additionally, we demonstrated that metastases can present with the newly introduced non-mass lesion in BI-RADS v2025[15], characterized by segmental distribution, heterogeneous echotexture with an echogenic rind. Furthermore, posterior acoustic enhancement was one of the hallmarks of the present study with 54.5% rate, likely reflecting the high cellularity and relative lack of internal desmoplasia in these metastatic deposits compared to the acoustic shadowing typical of primary breast cancers[3,16]. Interestingly, although the literature consistently emphasizes that metastases typically lack a desmoplastic reaction, thereby explaining the classical absence of spiculation[6,14], we observed a perilesional "echogenic rind" in 63.6% (14/22) of our dominant lesions, a finding that may represent a marker of peritumoral desmoplastic response commonly associated with malignant lesions. In the context of metastases, this feature may either reflect a true desmoplastic reaction or be secondary to rapid expansile growth causing compression of the adjacent adipose tissue. With respect to vascularity, internal and/or peripheral flow was detected on Doppler US in 83.3% (10/12) of the evaluated lesions, a rate substantially higher than that reported in the existing literature[3,16]. This discrepancy is likely attributable to two principal factors. First, the evolution of ultrasonographic technology is of critical importance. Contemporary high-frequency transducers and more sensitive Doppler software including advanced microvascular flow imaging techniques permit the detection of slow, low-volume vascular signals that would likely have fallen below the sensitivity threshold of older equipment used in earlier cohorts[21]. Second, the high prevalence of internal vascularity in our series may reflect robust neoangiogenesis associated with the specific, biologically aggressive primary tumors represented in our study population. Taken together, our findings suggest that metastases originating from solid tumors may be considerably more vascular than previously assumed, and that this vascularity is becoming increasingly detectable with advances in modern imaging technology. The present study demonstrated an almost equal distribution of hard and intermediate stiffness. While metastatic lesions are generally stiffer than benign masses, this distribution suggests that they may not uniformly reach the extreme stiffness levels frequently observed in high-grade primary invasive ductal carcinomas. This relative absence of extreme stiffness may be attributed to the lack of a dense, primary desmoplastic stromal reaction within the metastatic deposit itself[8]. Consequently, although elastography may aid in distinguishing metastases from benign lesions, our preliminary findings indicate that its utility in differentiating metastases from primary breast carcinomas appears to be limited.

While limited by our single-case MRI observation, the identified thick rim enhancement and low ADC value are noteworthy. This finding aligns with the 75.9% frequency of rim enhancement reported by Wienbeck et al. in metastatic lesions, a feature often attributed to central necrosis or rapid tumor growth. The low ADC value in our case reflects high cellularity, consistent with aggressive tumor biology[22]. However, as these observations are based on a single patient, they should be interpreted as illustrative rather than generalizable; further prospective studies with larger MRI cohorts are required to validate these imaging signatures.

Regarding clinical management, accurate BI-RADS assignment is essential. In our cohort, most lesions were classified as suspicious, with BI-RADS 4B being the most common (n=13), followed by 4C, 4A, 5, and 3. These results align with Wan et al., who assigned 85.7% of metastatic cases to category 4[16]. Most metastases lack pathognomonic imaging features, often overlapping with BI-RADS 4 or 5.

The primary limitations of this study include its descriptive design and a relatively small sample size, which reflects the inherent rarity of this condition; consequently, these factors constrain the scope of the statistical inferences that can be drawn. Furthermore, the extensive study period (2010–2026) may introduce heterogeneity regarding imaging technology and clinical protocols. However, these limitations provide a clear roadmap for future research. To enhance diagnostic precision, larger prospective multicenter studies are warranted to validate the diagnostic accuracy of the new BI-RADS v2025 descriptors across diverse patient populations. Future investigations should also prioritize the establishment of quantitative imaging thresholds, such as specific ADC values in MRI or kilopascal cut-offs in elastography, to provide more objective criteria for differentiating secondary metastases from aggressive primary breast cancers. Moreover, integrating these updated radiological patterns with the molecular or genetic profiling of the primary malignancy could facilitate a more personalized diagnostic approach, ultimately refining clinical management strategies.

In conclusion, metastases to the breast from extramammary solid tumors typically present as lobulated, hypoechoic masses with indistinct or obscured margin, often accompanied by posterior acoustic enhancement. The absence of internal calcifications remains a critical diagnostic clue. Radiologists must remain proficient in the BI-RADS v2025 descriptors to ensure timely and accurate diagnosis in this complex patient population.

Author Contributions: Concept/Design : UAP, HÖ; Data acquisition: UAP, HÖ; Data analysis and interpretation: UAP, HÖ; Drafting manuscript: UAP; Critical revision of manuscript: HÖ; Final approval and accountability: UAP, HÖ; Technical or material support: -; Supervision: UAP, HÖ; Securing funding (if available): n/a.
Ethical Approval: Ethical approval was obtained by the decision numbered 556472 dated 18.02.2026 issued by the Medical and Health Sciences Research Board of the Rectorate of Başkent University.
Peer-review: Externally peer-reviewed.
Conflict of Interest: Authors declared no conflict of interest.
Financial Disclosure: Authors declared no financial support

REFERENCES

1. Sedeta ET, Jobre B, Avezbakiyev B. Breast cancer: Global patterns of incidence, mortality, and trends. J Clin Oncol. 2023;41:10528.
2. Georgiannos SN, Chin Aleong J, Goode AW, Sheaff M. Secondary neoplasms of the breast. Cancer. 2001;92:2259-66.
3. Surov A, Fiedler E, Holzhausen HJ, Ruschke K, Schmoll HJ, Spielmann RP. Metastases to the breast from non-mammary malignancies. Acad Radiol. 2011;18:565-74.
4. DeLair DF, Corben AD, Catalano JP, Vallejo CE, Brogi E, Tan LK. Non-mammary metastases to the breast and axilla: a study of 85 cases. Mod Pathol. 2013;26:343-9.
5. Bitencourt AGV, Gama RRM, Graziano L, Negrão EMS, Sabino SMPS, Watanabe AHU et al. Breast metastases from extramammary malignancies: multimodality imaging aspects. Br J Radiol. 2017;90:20170197.
6. Bartella L, Kaye J, Perry NM, Malhotra A, Evans D, Ryan D et al. Metastases to the breast revisited: radiological-histopathological correlation. Clin Radiol. 2003;58:524-31.
7. Hejmadi RK, Day LJ, Young JA. Extramammary metastatic neoplasms in the breast: a cytomorphological study of 11 cases. Cytopathology. 2003;14:191-4.
8. Mun SH, Ko EY, Han BK, Shin JH, Kim SJ, Cho EY. Breast metastases from extramammary malignancies: typical and atypical ultrasound features. Korean J Radiol. 2014;15:20-8.
9. Li J, Wahab R, Brown AL, Guarnieri B, Lewis K, Mahoney MC et al. Extramammary metastases to the breast. Radiographics. 2023;43:230036.
10. Mariano L, Nicosia L, Latronico A, Pesapane F, Grimaldi E, Borella M et al. Metastatic breast involvement from extramammary malignancies: a review of dissemination pathways, imaging features, and management strategies. Radiol Med. 2025;130:1767-76.
11. Hajdu SI, Urban JA. Cancers metastatic to the breast. Cancer. 1972;29:1691-6.

12. Toombs BD, Kalisher L. Metastatic disease to the breast: clinical, pathologic, and radiographic features. AJR Am J Roentgenol. 1977;129:673-6.
13. Amichetti M, Perani B, Boi S. Metastases to the breast from extramammary malignancies. Oncology. 1990;47:257-60.
14. Sippo DA, Kulkarni K, Carlo PD, Lee B, Eisner D, Cimino-Mathews A et al. Metastatic disease to the breast from extramammary malignancies: a multimodality pictorial review. Curr Probl Diagn Radiol. 2016;45:225-32.
15. American College of Radiology. Breast Imaging Reporting and Data System (BI-RADS) v2025 Manual. Reston, VA, ACR. 2025.
16. Wan X, Zhang H, Zhang Y, Peng Y. Metastases to the breast from extramammary nonhematological malignancies: case series. Int J Gen Med. 2020;13:1105-14.
17. Noguera JJ, Martínez-Miravete P, Idoate F, Díaz L, Pina L, Zornoza G et al. Metastases to the breast: a review of 33 cases. Australas Radiol. 2007;51:133-8.
18. McCrea ES, Johnston C, Haney PJ. Metastases to the breast. AJR Am J Roentgenol. 1983;141:685-90.
19. Lee SK, Kim WW, Kim SH, Hur SM, Kim S, Choi JH et al. Characteristics of metastasis in the breast from extramammary malignancies. J Surg Oncol. 2010;101:137-40.
20. Bohman LG, Bassett LW, Gold RH, Voet R. Breast metastases from extramammary malignancies. Radiology. 1982;144:309-12.
21. Aziz MU, Eisenbrey JR, Deganello A, Zahid M, Sharbidre K, Sidhu P et al. Microvascular flow imaging: a state-of-the-art review of clinical use and promise. Radiology. 2022;305:250-64.
22. Wienbeck S, Herzog A, Kinner S, Surov A. Magnetic resonance imaging findings of intramammary metastases. Clin Imaging. 2016;40:361-4.